RSC Advances

PAPER

View Article Online
View Journal | View Issue

Cite this: *RSC Adv.*, 2024, **14**, 18444

BEDT-TTF radical-cation salts with tris(oxalato) chromate and guest additives†

Toby J. Blundell, [a] Joseph O. Ogar, [a] Michael J. Brannan,[a] Elizabeth K. Rusbridge,[a] John D. Wallis, [a] Hiroki Akutsu, [b] Yasuhiro Nakazawa,[b] Shusaku Imajo[c] and Lee Martin *[a]

Received 9th May 2024
Accepted 30th May 2024

DOI: 10.1039/d4ra03425b

rsc.li/rsc-advances

The family of radical-cation salts β″-(BEDT-TTF)$_4$[(A)M^{3+}(C$_2$O$_4$)$_3$]·guest (M = Fe, Cr, Ga, Al, Co, Mn, Rh, Ru; A = K$^+$, H$_3$O$^+$, NH$_4^+$) has produced superconductors, metals, semiconductors, and metal–insulators through introduction of different guest molecules into the structure. We present three new additions to the family β″-(BEDT-TTF)$_4$[(A)Cr(C$_2$O$_4$)$_3$]·guest with the guest molecules toluene, phenol, or salicylaldehyde. These new guests are liquid or solid additives within the electrocrystallisation medium. All three salts show metallic behaviour from room temperature down to <10 K and do not show a superconducting transition.

Introduction

Radical-cation salts of BEDT-TTF [bis(ethylenedithio)tetrathiafulvalene] with the tris(oxalato)metallate anion have produced a multitude of multifunctional materials which combine conductivity or superconductivity with paramagnetism,[1] ferromagnetism,[2] antiferromagnetism,[3] chirality,[4] or proton conductivity.[5] These salts consist of segregated stacks of conducting cationic BEDT-TTF layers and insulating anion layers. The packing arrangement of the BEDT-TTF donor molecules is determined by hydrogen-bonding interactions between the terminal ethylene groups of the BEDT-TTF molecules and the anion layer. Therefore, small changes to the structure of the anion layer will lead to changes in the BEDT-TTF donor packing arrangement and the conducting behaviour of the material.

The most widely studied in this family of salts are the 4 : 1 β″-(BEDT-TTF)$_4$[(A)M(C$_2$O$_4$)$_3$]·guest salts.[6] The anion layer in these salts consists of a honeycomb network of the counter cation (A = H$_3$O$^+$, NH$_4^+$, K$^+$) and the tris(oxalato)metallate anion (M(C$_2$O$_4$)$_3^{3-}$). Guest molecules are sited within the hexagonal cavities of the anion layer. The donor layer consists of BEDT-TTF$^{0.5+}$ molecules with close S···S contacts between donors in adjacent stacks. The first salt in this family to be discovered, and still the salt with the highest superconducting T_c (8.5 K) is β″-(BEDT-TTF)$_4$[(H$_3$O)Fe(C$_2$O$_4$)$_3$]·benzonitrile.[1] Shortly after this, the isostructural Cr(C$_2$O$_4$)$_3^{3-}$ salt was reported.[7] In the following years the metal centre has been changed to various 3d (Co^{3+},[8] Mn^{3+} (ref. 9)), 4d (Rh^{3+},[10] Ru^{3+} (ref. 11)), and main group (Al^{3+},[12] Ga^{3+} (ref. 13)) metal ions. Changes to the size of the metal ion and the distance between the oxalate oxygens and the cation (A = H$_3$O$^+$, NH$_4^+$, K$^+$) determine the size of the anion layer hexagons within which the guests are located. The resulting size change has been shown to have a small effect on the conducting behaviour whereas a much more pronounced effect is observed by changing the size and shape of the included guest molecule which is sited within the hexagonal cavities. The –C≡N bond of the benzonitrile guest molecules are aligned along the *b* axis[1] and a correlation has been observed between the length of the *b* axis and the superconducting T_c.[14] Longer molecules such as benzonitrile, nitrobenzene, or bromobenzene give superconductors with higher T_cs, whilst smaller molecules such as fluorobenzene have a shorter *b* axis and remain metallic without showing a superconducting transition.[14] Using even smaller guests such as nitromethane can lead to a different phase which is a 3 : 1 semiconducting phase.[15] Using larger guests such as sec-phenethyl alcohol[4] or 1,2-dibromobenzene[16] leads to the guest molecules being arranged asymmetrically in the anion layer and interacting differently with each of the two neighbouring donor layers. This produces a 4 : 1 bilayered salt with two different donor packing types α and β″,[4,17] or α and pseudo-κ.[16]

When the guest is benzonitrile a second 4 : 1 polymorph is also obtained which has the same formula, (BEDT-TTF)$_4$[(H$_3$O)M(C$_2$O$_4$)$_3$]·benzonitrile.[18] In this case, the donors pack in a very

[a]*School of Science and Technology, Nottingham Trent University, Clifton Lane, Clifton, Nottingham, NG11 8NS, UK. E-mail: lee.martin@ntu.ac.uk*

[b]*Department of Chemistry, Graduate School of Science, Osaka University, 1-1 Machikaneyama-cho, Toyonaka, Osaka 560-0043, Japan*

[c]*The Institute for Solid State Physics, The University of Tokyo, Kashiwa, Chiba 277-8581, Japan*

† CCDC 2338454–2338456 contains supplementary X ray crystallographic data for (**I**), (**II**) and (**III**) respectively . This data can be obtained free of charge. For crystallographic data in CIF or other electronic format see DOI: https://doi.org/10.1039/d4ra03425b

different way with $(BEDT\text{-}TTF^{+})_2$ dimers each surrounded by six neutral BEDT-TTF monomers to give a semiconductor. The anion layer of this 'pseudo-κ' phase and that of the superconducting β″ phase differ in the distribution of the Δ and Λ enantiomers of the $M(C_2O_4)_3^{3-}$ anion which leads to the benzonitrile molecule being disordered over two positions in the pseudo-κ phase.[18]

2 : 1 superconductors,[19] semiconductors,[20] and proton conductors[5] have been obtained where the included guest molecule is the 18-crown-6 ether used to aid solubility of the anion, rather than the solvents which have been used in the electrocrystallisation.

The origin of the superconductivity in this family of salts is of interest owing to its unconventional mechanism[21] and in the search for new superconductors we present the crystal structures and electrical resistance measurements for three new radical-cation salts in the family β″-(BEDT-TTF)$_4$[(A)Cr$(C_2O_4)_3$]·guest (A = $K^+/H_3O^+/NH_4^+$). These guests toluene, phenol, or salicylaldehyde are a liquid or solid additive within the electrocrystallisation medium 1,2,4-trichlorobenzene:ethanol (Scheme 1).

Results and discussion

β″-(BEDT-TTF)$_4$[$(NH_4)Cr(C_2O_4)_3$]·toluene (I)

Salt (**I**) crystallises in monoclinic space group *C*2/*c* with an asymmetric unit consisting of two crystallographically independent BEDT-TTF donors, half a tris(oxalato)chromate anion, half a toluene molecule, and half an NH_4^+ cation. Fig. 1 shows the alternating donor and anion layers viewed down the *a* axis. The crystallographically independent A and B donors adopt a β″ packing motif (Fig. 2) with an …AABBAABB… packing mode within a donor stack. There are several side-to-side S···S close contacts between donor stacks similar to those observed in other salts in this family of 4 : 1 β″ salts (Table 1).[6] Table 2

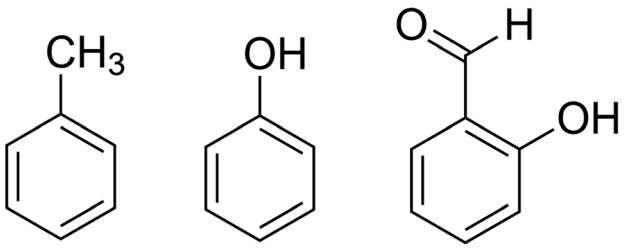

Scheme 1 From left to right, toluene, phenol, and salicylaldehyde.

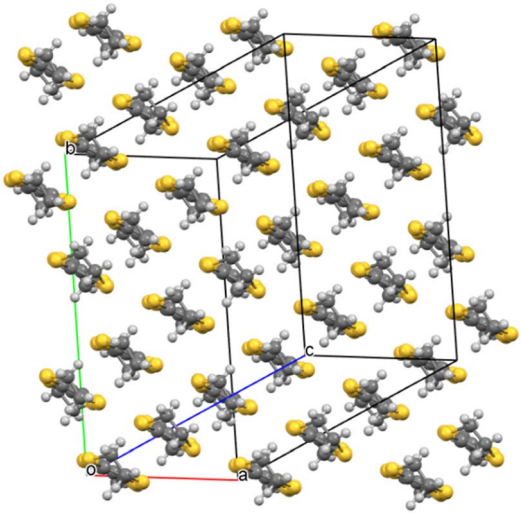

Fig. 2 Donor layer of β″-(BEDT-TTF)$_4$[$(NH_4)Cr(C_2O_4)_3$]·toluene (I).

Table 1 Short S···S contacts (<sum VdW radii) for β″-(BEDT-TTF)$_4$[$(NH_4)Cr(C_2O_4)_3$]·toluene (I)

S atom 1	S atom 2	Contact (Å)
S9	S13	3.459(2)
S9	S16	3.391(3)
S10	S1	3.488(3)
S11	S1	3.459(2)
S15	S6	3.349(2)
S15	S8	3.290(3)
S16	S1	3.592(3)
S10	S7	3.545(3)

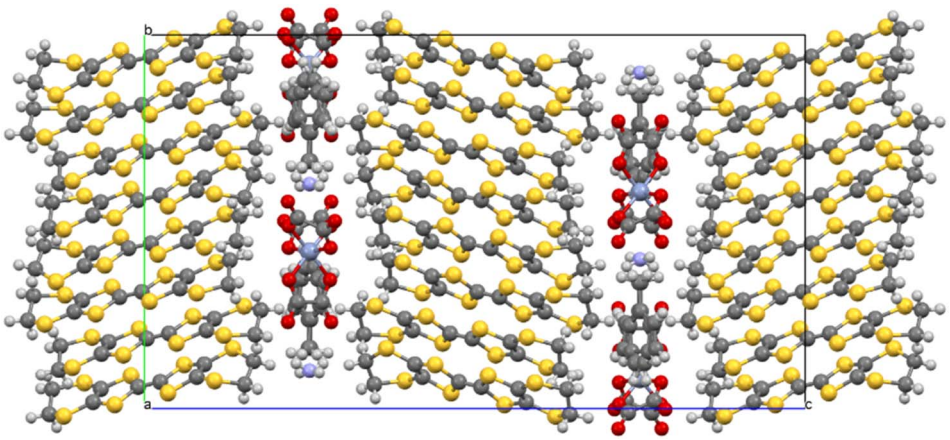

Fig. 1 Layered packing of β″-(BEDT-TTF)$_4$[$(NH_4)Cr(C_2O_4)_3$]·toluene (I) viewed down the *a* axis.

Table 2 Approximation of the charge of BEDT-TTF molecules in β″-(BEDT-TTF)$_4$[(NH$_4$)Cr(C$_2$O$_4$)$_3$]·toluene (I) based on the bond lengths (Å):[22] $\delta = (b + c) - (a + d)$, $Q = 6.347 - 7.463\delta$

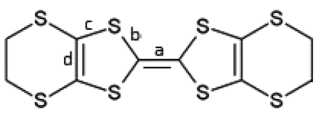

Donor	*a*	*b*	*c*	*d*	*δ*	*Q*
A	1.356	1.7425	1.74625	1.354	0.779	0.54^+
B	1.351	1.74375	1.7505	1.3565	0.787	0.48^+

shows the estimation of charges on the BEDT-TTF molecules are close to the expected 0.5^+ based on the method of Guionneau *et al.*[22]

The honeycomb arrangement of the anion layer is show in Fig. 3. The hexagonal cavities created by the tris(oxalato)chromate anions and NH_4^+ cations contain disordered toluene guest molecules. The $-CH_3$ group of the toluene is directed towards a Cr metal centre along the *b* axis (Fig. 3). A single anion layer consists only of a single enantiomer of $Cr(C_2O_4)_3^{3-}$ with the next anion layer consisting of only the other enantiomer, to give a salt which is racemic overall.

The electrical resistance of salt (**I**) (Fig. 4) shows metallic behaviour down to 1.8 K with no transition to the superconducting state.

β″-(BEDT-TTF)$_4$[(H$_3$O)Cr(C$_2$O$_4$)$_3$].phenol (II)

Salt (**II**) is isostructural with (**I**) and incorporates phenol as the guest molecule (Fig. 5–7). Short S⋯S contacts are given in Table 3. Table 4 shows the estimated charges of the two crystallographically independent BEDT-TTF molecules, which in this case are slightly higher than the expected 0.5^+. The anion layer for (**II**) has a hexagonal arrangement of $Cr(C_2O_4)_3^{3-}$ and H_3O^+ cations with phenol guest molecules within the honeycomb cavities (Fig. 7). In the β″-(BEDT-TTF)$_4$[(A)M(C$_2$O$_4$)$_3$]· guest family (A = K^+/H_3O^+/NH_4^+) the guest molecule is usually a monosubstituted benzene with the R group directed along the *b* axis towards the metal centre of the tris(oxalato)metallate anion, as is the case for Cr/toluene (Fig. 3). However, in salt (**II**) the –OH group of the phenol guest molecules are disordered over two positions and not along the *b* axis (Fig. 7). The electrical resistance of salt (**II**) (Fig. 8) shows metallic behaviour down to 0.5 K with no transition to the superconducting state. There is a slight upturn in the resistivity below 4 K.

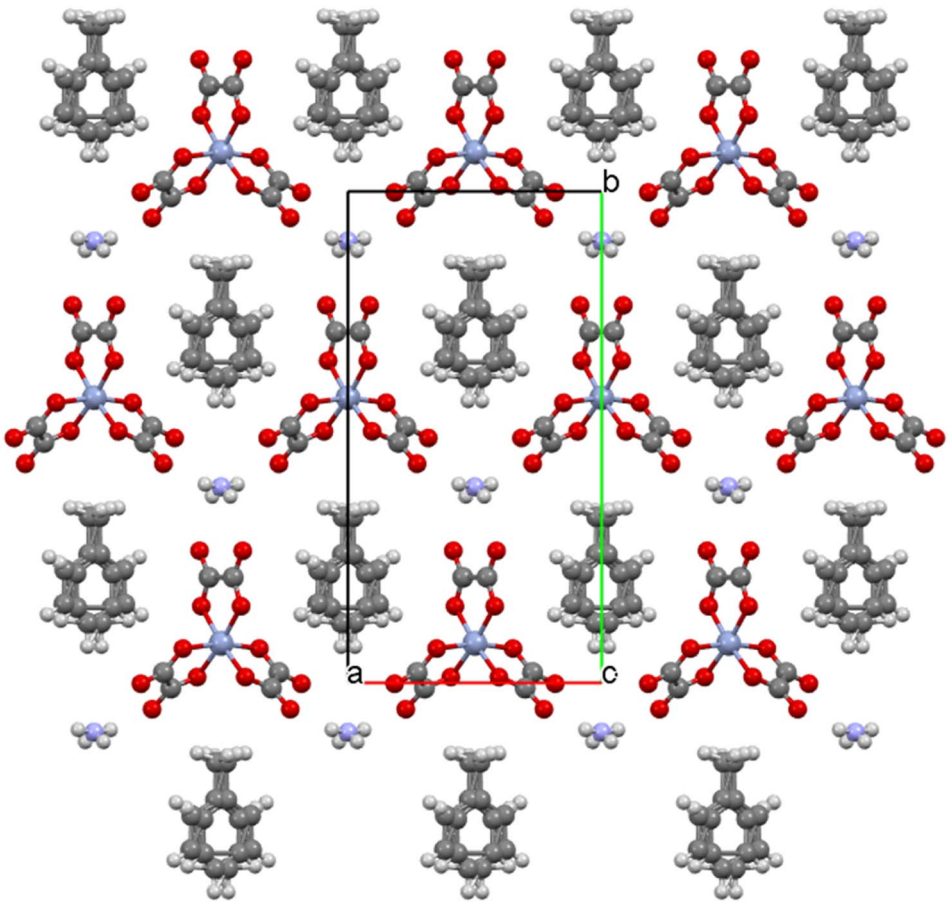

Fig. 3 Anion layer of β″-(BEDT-TTF)$_4$[(NH$_4$)Cr(C$_2$O$_4$)$_3$]·toluene (I) viewed down the *c* axis.

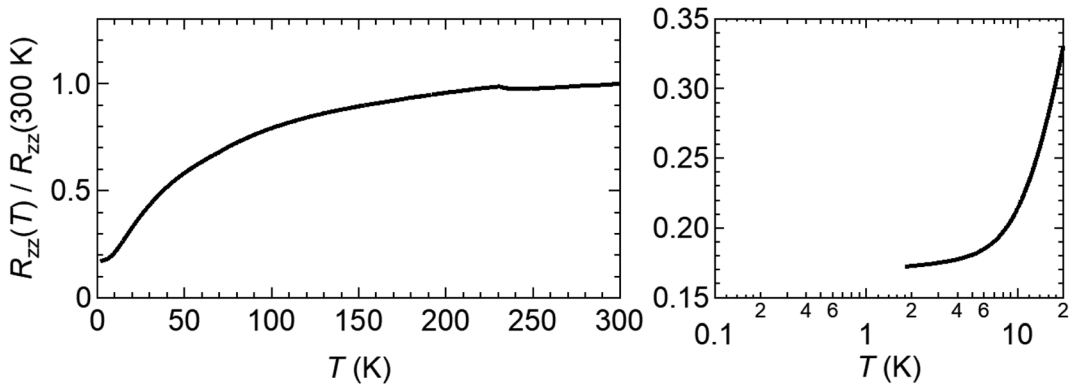

Fig. 4 Electrical resistance of β″-(BEDT-TTF)$_4$[(NH$_4$)Cr(C$_2$O$_4$)$_3$]·toluene (**I**). The resistance below 10 K is shown on the right-hand side.

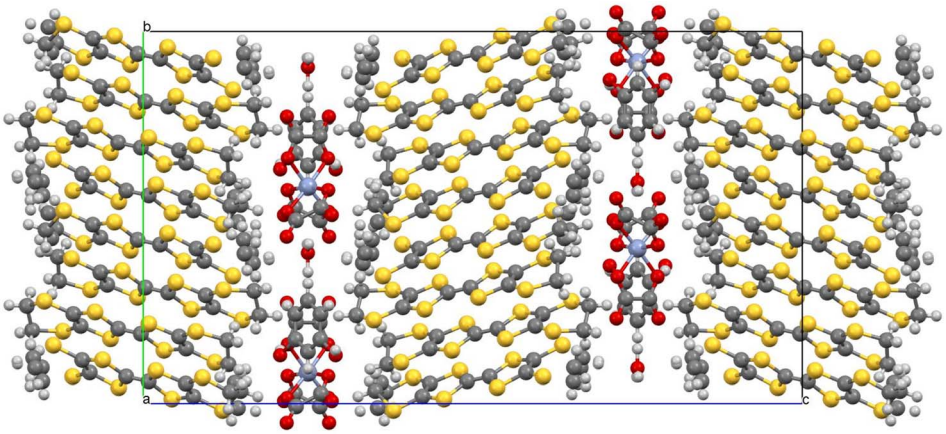

Fig. 5 Layered packing of β″-(BEDT-TTF)$_4$[(H$_3$O)Cr(C$_2$O$_4$)$_3$]·phenol (**II**) viewed down the *a* axis.

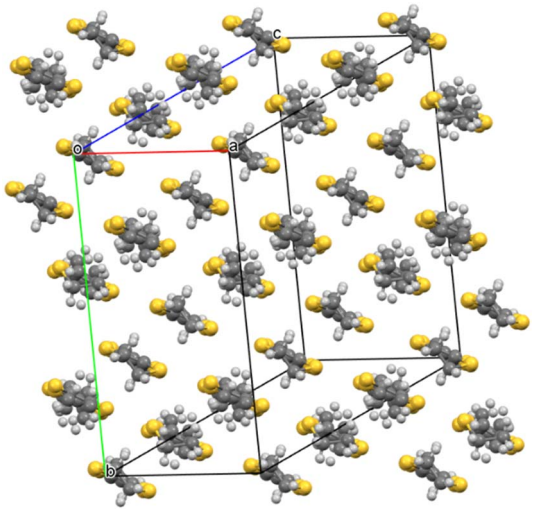

Fig. 6 Donor layer of β″-(BEDT-TTF)$_4$[(H$_3$O)Cr(C$_2$O$_4$)$_3$]·phenol (**II**).

β″-(BEDT-TTF)$_4$[(H$_3$O)Cr(C$_2$O$_4$)$_3$]·salicylaldehyde (III)

Salt (**III**) is isostructural with (**I**) and (**II**) and incorporates the larger salicylaldehyde as the guest molecule. The salicylaldehyde molecule is heavily disordered within the honeycomb cavities. Short S···S contacts are given in Table 5. Table 6 shows the estimated charges of the two crystallographically independent BEDT-TTF molecules, which in this case are slightly lower than the expected 0.5$^+$. The electrical resistance of salt (**III**) (Fig. 9) shows metallic behaviour down to 0.5 K with no transition to the superconducting state. There is a slight upturn in the resistivity below 4 K.

Relationship of the *b* axis length to the superconducting T_c[14]

Salts (**I**)–(**III**) are isostructural with the salts presented in Table 7 which shows the conducting properties and the *b* axis length for each salt in the family β″-(BEDT-TTF)$_4$[(A)Cr(C$_2$O$_4$)$_3$]·guest (A = K$^+$/H$_3$O$^+$/NH$_4^+$). There are three superconducting salts with Cr(C$_2$O$_4$)$_3$ where the guest molecule is benzonitrile[7] (T_c = 5.5–6.0 K), nitrobenzene[23] (T_c = 5.8 K), or bromobenzene[24] (T_c = 1.5

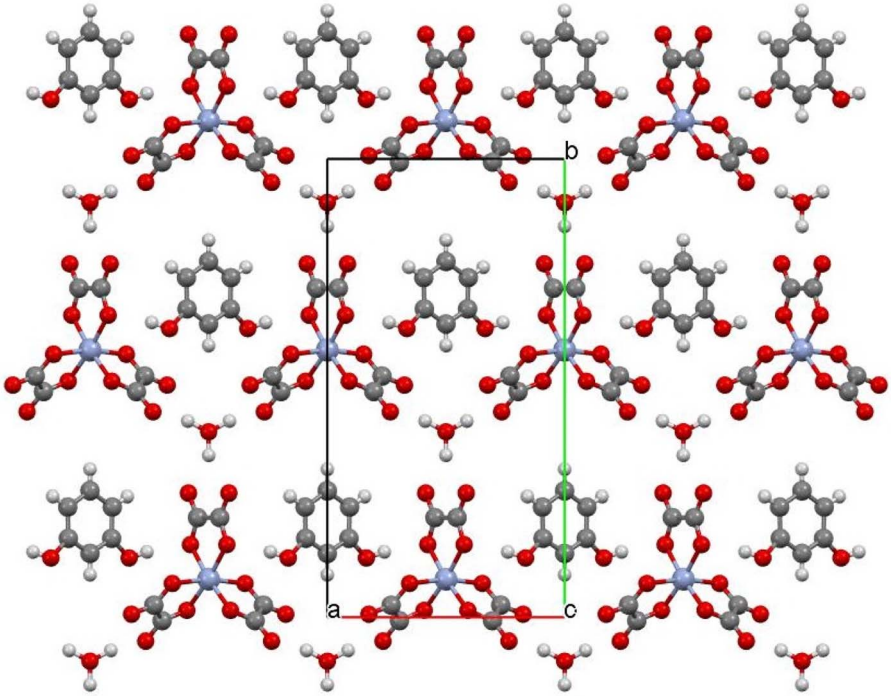

Fig. 7 Anion layer of β″-(BEDT-TTF)$_4$[(H$_3$O)Cr(C$_2$O$_4$)$_3$]·phenol (**II**) viewed down the *c* axis.

Table 3 Short S⋯S contacts (<sum VdW radii) for β″-(BEDT-TTF)$_4$[(H$_3$O)Cr(C$_2$O$_4$)$_3$].phenol (**II**)

S atom 1	S atom 2	Contact (Å)
S1	S7	3.5312(9)
S5	S7	3.3940(9)
S4	S15	3.5391(9)
S6	S9	3.3977(9)
S6	S13	3.3629(9)

Table 4 Approximation of the charge of BEDT-TTF molecules in β″-(BEDT-TTF)$_4$[(H$_3$O)Cr(C$_2$O$_4$)$_3$]·phenol (**II**) based on the bond lengths (Å):[22] $\delta = (b + c) - (a + d)$, $Q = 6.347 - 7.463\delta$

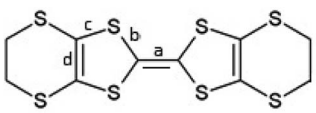

Donor	*a*	*b*	*c*	*d*	*δ*	*Q*
A	1.369	1.741	1.74925	1.3525	0.769	0.61^+
B	1.371	1.73725	1.74725	1.3535	0.760	0.68^+

K). The –C≡N, –NO$_2$, or –Br group in these superconductors is directed along the *b* axis and increased length of the guest molecule and *b* axis has been correlated with an increase in the superconducting T_c.[14] With slightly smaller guest molecules the *b* axis is reduced and no transition to the superconducting state is observed. The choice of guests has previously been confined to those which can act as the solvent for growth of the crystals *via* electrocrystallisation. Incorporating a guest which is an additive to the crystal growing solvent gives many new possibilities for guests that may increase the *b* axis length and the superconducting T_c to aid with the study of the unconventional mechanism of superconductivity in these salts.[29] There is also the possibility of adding extra functionality to the material *via* the guest additive.

Salts (**I**)–(**III**) all show metallic behaviour with no transition to the superconducting state, and salts (**II**) and (**III**) show an upturn in the resistance below 10 K. This upturn has also observed in the metallic salts Cr/dimethylformamide,[25] Cr/2-bromopyridine[26] and Cr/2-chloropyridine.[26] The *b* axes for Cr/toluene (**I**) and Cr/phenol (**II**) are shorter than those of the three superconducting salts Cr/benzonitrile, Cr/nitrobenzene, and Cr/bromobenzene, which explains the lack of a superconducting transition in (**I**) and (**II**). However, the *b* axis length of 19.970(3) Å for Cr/salicylaldehyde (**III**) is longer at room temperature than the superconducting Cr/bromobenzene ($T_c = 1.5$ K, $b = 19.9773(11)$ Å).

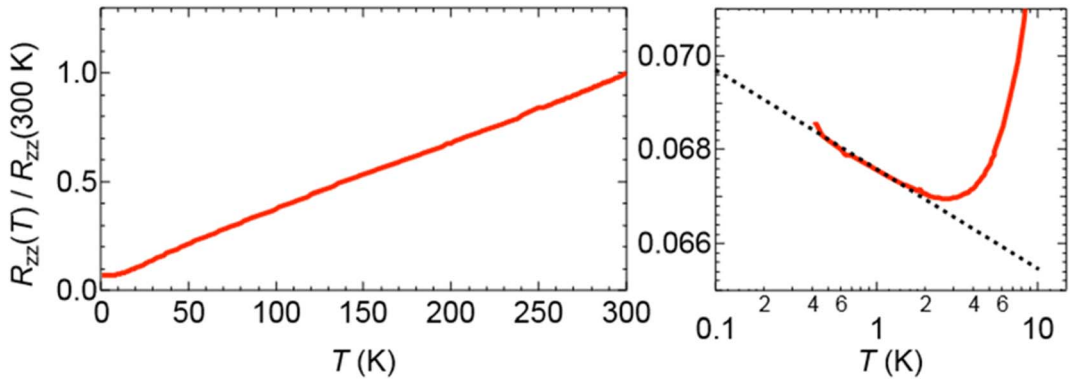

Fig. 8 Electric resistance of β″-(BEDT-TTF)$_4$[(H$_3$O)Cr(C$_2$O$_4$)$_3$]·phenol (**II**). The upturn in resistance below 10 K is shown on the right-hand side.

Table 5 Short S⋯S contacts (<sum VdW radii) for β″-(BEDT-TTF)$_4$[(H$_3$O)Cr(C$_2$O$_4$)$_3$]·salicylaldehyde (**III**)

S atom 1	S atom 2	Contact (Å)
S1	S7	3.414(6)
S3	S7	3.509(7)
S2	S9	3.373(6)
S2	S11	3.422(7)
S6	S15	3.558(7)
S8	S10	3.589(8)

Table 6 Approximation of the charge of BEDT-TTF molecules in β″-(BEDT-TTF)$_4$[(H$_3$O)Cr(C$_2$O$_4$)$_3$]·salicylaldehyde (**III**) based on the bond lengths (Å):[22] $\delta = (b + c) - (a + d)$, $Q = 6.347 - 7.463\delta$

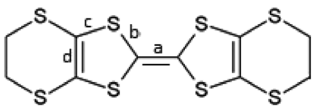

Donor	*a*	*b*	*c*	*d*	*δ*	*Q*
A	1.261	1.769	1.72975	1.338	0.900	0.37$^+$
B	1.309	1.76325	1.75325	1.412	0.795	0.41$^+$

The lack of a superconducting transition and an upturn in resistance below 10 K has previously been observed in Cr/2-bromopyridine and Cr/2-chloropyridine.[26] This is in contrast to their superconducting Fe analogues[30] and has been attributed to disorder in the tris(oxalato)metallate anions and in the K^+/H_3O^+ cations of the anion layers. Salicylaldehyde is a non-symmetrical guest and it has been previously been concluded that ordering of a non-symmetrical guest may stop it becoming superconducting due to the dipole moment.[31]

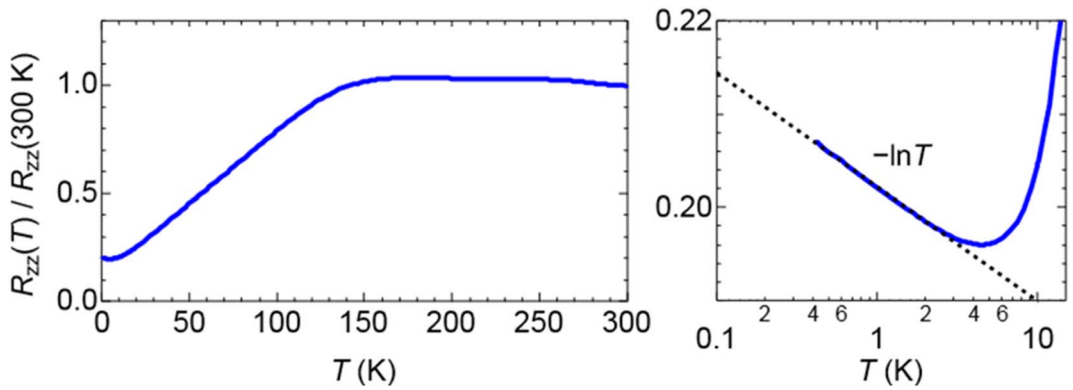

Fig. 9 Electrical resistance of β″-(BEDT-TTF)$_4$[(H$_3$O)Cr(C$_2$O$_4$)$_3$]·salicylaldehyde (**III**). The upturn in resistance below 10 K is shown on the right-hand side.

Table 7 Relationship of the *b* axis length with conducting properties for the family of salts β″-(BEDT-TTF)$_4$[(A)Cr(C$_2$O$_4$)$_3$]·guest (A = K$^+$/H$_3$O$^+$/NH$_4^+$)

Guest	A$^+$	Conductivity	*b* axis at room temperature/Å	*b* axis at lower temperature/Å	Ref.
Toluene (**I**)	NH_4^+	Metal >4.2 K		19.8060(2) [120 K]	
Phenol (**II**)	H_3O^+	Metal >4.2 K	19.9211(4)		
Salicylaldehyde (**III**)	H_3O^+	Metal >4.2 K	19.970(3)		
Benzonitrile	H_3O^+	T_c = 5.5–6.0 K	20.130(4)	19.965(1) [120 K]	7
Nitrobenzene	H_3O^+/NH_4^+	T_c = 5.8 K	20.0908(3)	19.91720(10) [120 K]	23
Bromobenzene	H_3O^+	T_c = 1.5 K	19.9773(11)		24
Dimethylformamide	K^+/NH_4^+	Metal >4.2 K	19.888(2)		25
Dimethylformamide	K^+	Metal >4.2 K	19.880(3)		25
2-Bromopyridine	H_3O^+/K^+	Metal >0.5 K	20.0382(5)		26
2-Chloropyridine	H_3O^+/K^+	Metal >0.5 K	20.0020(9)		26
Pyridine	H_3O^+	Metal >0.5 K	19.965		27
Chlorobenzene	H_3O^+	Metal >130 K	19.9420(10)		20
Dichloromethane	H_3O^+	Semicon <150 K		19.7144(11) [150 K]	28

Conclusions

We present three new additions to the family β″-(BEDT-TTF)$_4$[(A)Cr(C$_2$O$_4$)$_3$]·guest with the guest molecules toluene, phenol, or salicylaldehyde. These new guests are a liquid or solid additive within the electrocrystallisation medium. Previously guests had been limited to those acting as the solvents for crystal growth. This offers new possibilities for inclusion of guests which can add extra functionality to the material or extend the length of the *b* axis to increase the superconducting T_c. All three salts show metallic behaviour from room temperature down to <10 K, and the phenol and salicylaldehyde salts show an upturn in resistance below 10 K. The *b* axis length in this family of salts shows a correlation with the conducting properties. Salt (**III**) (Cr/salicylaldehyde) has a comparable *b* axis length to superconducting Cr/bromobenzene (T_c = 1.5 K), whilst salts (**I**) and (**II**) have shorter *b* axes to explain their metallic behaviour. Salicylaldehyde is a non-symmetrical guest and its dipole moment may be the reason that it does not show superconductivity.

Experimental

Starting materials

Ammonium tris(oxalato)chromate was synthesized by the method of Bailar and Jones.[32] 1,2,4-Trichlorobenzene, ethanol, phenol, toluene, salicylaldehyde and 18-crown-6 ether were purchased from Sigma-Aldrich and used as received. BEDT-TTF was purchased from TCI and recrystallised from chloroform.

Synthesis of radical-cation salts

Salt (**I**) was synthesised by adding 100 mg of ammonium tris(oxalato)chromate, 250 mg 18-crown-6 ether, and 10 ml of toluene to 15 ml 1,2,4-trichlorobenzene : 3 ml ethanol and stirring overnight before filtering into a H-cell containing 10 mg BEDT-TTF in the anode side. A current of 0.5 μA was applied to give black blocks which were collected after 1 month.

Salt (**II**) was synthesised by adding 100 mg of ammonium tris(oxalato)chromate, 250 mg 18-crown-6 ether, and 100 mg of phenol to 15 ml 1,2,4-trichlorobenzene : 3 ml ethanol and stirring overnight before filtering into a H-cell containing 10 mg BEDT-TTF in the anode side. A current of 0.5 μA was applied for 3 weeks to give black blocks.

Salt (**III**) was synthesised by adding 100 mg of ammonium tris(oxalato)chromate, 200 mg 18-crown-6 ether, and 10 ml of salicylaldehyde to 10 ml 1,2,4-trichlorobenzene : 2 ml ethanol and stirring overnight before filtering into a H-cell containing 10 mg BEDT-TTF in the anode side. A current of 0.5 μA was applied for 3 weeks to give black blocks.

Electrical resistivity measurements

Temperature dependent electrical resistivity measurements were performed using four contacts on single crystals of (**I**), (**II**) and (**III**).

X-ray crystallography

Data were collected on a Rigaku Oxford Diffraction XtaLAB Synergy R, DW system, HyPix-Arc 100 using CuKα radiation at 150 K for (**I**) using CrystalisPro software.[33]

Data were collected on a Rigaku R-AXIS VII imaging plate system with FR-E SuperBright High-Brilliance Rotating Anode Generator with confocal monochromated MoKα radiation, using Rapid Auto software for control and processing at 298 K for (**II**) and (**III**).

The crystal structure for (**I**) was solved and refined using Olex2 (ref. 34) with SHELXT 2018/2 (ref. 35) (solution) and SHELXL 2019/2 (ref. 36) (refinement).

The crystal structure for (**II**) was solved and refined using Olex2 (ref. 34) with SHELXT 2018/2(ref. 35) (solution) and SHELXL 2018/3(ref. 37) (refinement).

The crystal structure for (**III**) was solved with SIR2014 (ref. 38) and refined with SHELXL 2018/3.[37] The heavily disordered guest molecules in the hexagonal cavity which could not be resolved were removed from calculations using SQUEEZE from the PLATON program.[39]

All molecular illustrations were prepared using Mercury.[40]

Crystal data for (I). At 120 K: $C_{53}H_{42}CrNO_{12}S_{32}$, M = 1962.79, black block, a = 10.2438(1), b = 19.8060(2), c = 35.2267(3) Å, β = 94.350(1)°, U = 7126.51(12) Å^3, T = 119.99(10) K, space group

$C2/c$, $Z = 4$, $\mu = 10.606$ mm^{-1}, reflections collected = 202 853, independent reflections = 7477, $R1 = 0.0877$, w$R2 = 0.1835$ [$F^2 > 2\sigma(F^2)$], $R1 = 0.0885$, w$R2 = 0.1839$ (all data). CCDC 2338454.

Crystal data for (II). At 298 K: $C_{52}H_{39}CrO_{14}S_{32}$, $M = 1965.79$, black block, $a = 10.3270(2)$, $b = 19.9211(4)$, $c = 35.3072(7)$ Å, $\beta = 93.139(7)°$, $U = 7252.7(2)$ Å^3, $T = 298$ K, space group $C2/c$, $Z = 4$, $\mu = 1.140$ mm^{-1}, reflections collected = 34 185, independent reflections = 8299, $R1 = 0.0391$, w$R2 = 0.0457$ [$F^2 > 2\sigma(F^2)$], $R1 = 0.1044$, w$R2 = 0.1091$ (all data). CCDC 2338455.

Crystal data for (III). At 298 K: $C_{53}H_{39}CrO_{15}S_{32}$, $M = 1993.80$, black block, $a = 10.3201(11)$, $b = 19.970(3)$, $c = 35.467(4)$ Å, $\beta = 92.995(7)°$, $U = 7299.5(15)$ Å^3, $T = 298$ K, space group $C2/c$, $Z = 4$, $\mu = 1.135$ mm^{-1}, reflections collected = 31 619, independent reflections = 8283, $R1 = 0.2301$, w$R2 = 0.5352$ [$F^2 > 2\sigma(F^2)$], $R1 = 0.2843$, w$R2 = 0.5535$ (all data). CCDC 2338456.

Author contributions

Synthesis MB, EKR, LM; X-ray crystallography, HA, TJB, JOO, LM; conductivity measurements SI, HA, YN, EKR; writing – original draft preparation, LM; project administration, LM; funding acquisition, LM; supervision, LM, JDW, TJB, JOO.

Conflicts of interest

There are no conflicts to declare.

Acknowledgements

LM, JOO and TJB would like to thank the Leverhulme Trust for financial support (RPG-2019-242). EKR would like to thank NTU for a PhD studentship. EKR, LM, HA, and YN would like to thank JSPS for funding the Summer Program for EKR.

References

1 A. W. Graham, M. Kurmoo and P. Day, *J. Chem. Soc., Chem. Commun.*, 1995, 2061–2062; M. Kurmoo, A. W. Graham, P. Day, S. J. Coles, M. B. Hursthouse, J. L Caulfield, J. Singleton, F. L. Pratt and W. Hayes, *J. Am. Chem. Soc.*, 1995, **117**, 12209–12217.

2 E. Coronado, J. R. Galán-Mascarós, C. J. Gómez-García and V. Laukhin, *Nature*, 2000, **408**, 447–449.

3 B. Zhang, Y. Zhang and D. Zhu, *Chem. Commun.*, 2012, **48**, 197–199.

4 L. Martin, P. Day, H. Akutsu, J.-i. Yamada, S.-i. Nakatsuji, W. Clegg, R. W. Harrington, P. N. Horton, M. B. Hursthouse, P. McMillan and S. Firth, *CrystEngComm*, 2007, **10**, 865–867.

5 A. Akutsu-Sato, H. Akutsu, S. S. Turner, P. Day, M. R. Probert, J. A. K. Howard, T. Akutagawa, S. Takeda, T. Nakamura and T. Mori, *Angew. Chem., Int. Ed.*, 2005, **44**, 291–295.

6 L. Martin, *Coord. Chem. Rev.*, 2018, **376**, 277–291; S. Benmansour and C. J. Gómez-García, *Magnetochemistry*, 2021, **7**, 93.

7 L. Martin, S. S. Turner, P. Day, K. M. A. Malik, S. J. Coles and M. B. Hursthouse, *J. Chem. Soc., Chem. Commun.*, 1999, 513–514.

8 L. Martin, S. S. Turner, P. Day, P. Guionneau, J. A. K. Howard, D. E. Hibbs, M. E. Light, M. B. Hursthouse, M. Uruichi and K. Yakushi, *Inorg. Chem.*, 2001, **40**, 1363–1371.

9 S. Benmansour, Y. Sánchez-Máñez and C. J. Gómez-García, *Magnetochemistry*, 2017, **3**, 7.

10 L. Martin, A. L. Morritt, J. R. Lopez, Y. Nakazawa, H. Akutsu, S. Imajo, Y. Ihara, B. Zhang, Y. Zhang and Y. Guo, *Dalton Trans.*, 2017, **46**, 9542–9548.

11 T. G. Prokhorova, L. V. Zorina, S. V. Simonov, V. N. Zverev, E. Canadell, R. P. Shibaeva and E. B. Yagubskii, *CrystEngComm*, 2013, **15**, 7048.

12 T. J. Blundell, M. Brannan, J. Mburu-Newman, H. Akutsu, Y. Nakazawa, S. Imajo and L. Martin, *Magnetochemistry*, 2021, **7**, 90.

13 T. J. Blundell, A. L. Morritt, E. K. Rusbridge, L. Quibell, J. Oakes, H. Akutsu, Y. Nakazawa, S. Imajo, T. Kadoya, J.-i. Yamada, S. J. Coles, J. Christensen and L. Martin, *Mater. Adv.*, 2022, **3**, 4724–4735.

14 S. Imajo, H. Akutsu, A. Akutsu-Sato, A. L. Morritt, L. Martin and Y. Nakazawa, *Phys. Rev. Res.*, 2019, **1**, 033184.

15 L. Martin, H. Akutsu, P. N. Horton and M. B. Hursthouse, *CrystEngComm*, 2015, **17**, 2783–2790; L. Martin, S.-i. Nakatsuji, J.-i. Yamada, H. Akutsu and P. Day, *J. Mater. Chem.*, 2010, **20**, 2738–2742; L. Martin, P. Day, S.-i. Nakatsuji, J.-i. Yamada, H. Akutsu and P. Horton, *CrystEngComm*, 2010, **12**, 1369–1372.

16 L. V. Zorina, S. S. Khasanov, S. V. Simonov, R. P. Shibaeva, V. N. Zverev, E. Canadell, T. G. Prokhorova and E. B. Yagubskii, *CrystEngComm*, 2011, **13**, 2430–2438.

17 H. Akutsu, A. Akutsu-Sato, S. S. Turner, P. Day, E. Canadell, S. Firth, R. J. H. Clark, J. Yamada and S. Nakatsuji, *Chem. Commun.*, 2004, 18–19.

18 L. Martin, S. S. Turner, P. Day, F. E. Mabbs and E. J. L. McInnes, *J. Chem. Soc., Chem. Commun.*, 1997, 1367–1368.

19 L. Martin, A. L. Morritt, J. R. Lopez, H. Akutsu, Y. Nakazawa, S. Imajo and Y. Ihara, *Inorg. Chem.*, 2017, **56**(2), 717–720; L. Martin, J. R. Lopez, H. Akutsu, Y. Nakazawa and S. Imajo, *Inorg. Chem.*, 2017, **56**(22), 14045–14052.

20 A. L. Morritt, J. R. Lopez, T. J. Blundell, E. Canadell, H. Akutsu, Y. Nakazawa, S. Imajo and L. Martin, *Inorg. Chem.*, 2019, **58**, 10656–10664.

21 S. Imajo, H. Akutsu, R. Kurihara, T. Yajima, Y. Kohama, M. Tokunaga, K. Kindo and Y. Nakazawa, *Phys. Rev. Lett.*, 2020, **125**, 177002.

22 P. Guionneau, C. J. Kepert, G. Bravic, D. Chasseau, M. R. Truter, M. Kurmoo and P. Day, *Synth. Met.*, 1997, **86**, 1973–1974.

23 S. Rashid, S. S. Turner, P. Day, J. A. K. Howard, P. Guionneau, E. J. L. McInnes, F. E. Mabbs, R. J. H. Clark, S. Firth and T. Biggs, *J. Mater. Chem.*, 2001, **11**, 2095–2101.

24 E. Coronado, S. Curreli, C. Gimenez-Saiz and C. J. Gómez-García, *Synth. Met.*, 2005, **154**, 245–248.

25 T. G. Prokhorova, S. S. Khasanov, L. V. Zorina, L. I. Buravov, V. A. Tkacheva, A. A. Baskakov, R. B. Morgunov, M. Gener, E. Canadell, R. P. Shibaeva and E. B. Yagubskii, *Adv. Funct. Mater.*, 2003, **13**, 403–411.
26 T. G. Prokhorova, E. B. Yagubskii, L. V. Zorina, S. V. Simonov, V. N. Zverev, R. P. Shibaeva and L. I. Buravov, *Crystals*, 2018, **8**, 92.
27 A. I. Coldea, A. F. Bangura, J. Singleton, A. Ardavan, A. Akutsu-Sato, H. Akutsu, S. S. Turner and P. Day, *Phys. Rev. B: Condens. Matter Mater. Phys.*, 2004, **69**, 085112.
28 S. Rashid, S. S. Turner, D. Le Pevelen, P. Day, M. E. Light, M. B. Hursthouse, S. Firth and R. J. H. Clark, *Inorg. Chem.*, 2001, **40**, 5304–5306.
29 Y. Ihara and S. Imajo, *Crystals*, 2022, **12**(5), 711.
30 T. G. Prokhorova, L. I. Buravov, E. B. Yagubskii, L. V. Zorina, S. V. Simonov, V. N. Zverev, R. P. Shibaeva and E. Canadell, *Eur. J. Inorg. Chem.*, 2015, **34**, 5611–5620.
31 T. G. Prokhorova, E. B. Yagubskii, A. A. Bardin, V. N. Zverev, G. V. Shilov and L. I. Buravov, *Magnetochemistry*, 2021, **7**, 83.
32 J. C. Bailar and E. M. Jones, *Inorg. Synth.*, 1939, **1**, 35.
33 Agilent, *CrysAlis PRO*, Agilent Technologies Ltd, Yarnton, Oxfordshire, England, 2014.
34 O. V. Dolomanov, L. J. Bourhis, R. J. Gildea, J. A. K. Howard and H. Puschmann, *J. Appl. Crystallogr.*, 2009, **42**, 339–341.
35 G. M. Sheldrick, *Acta Crystallogr.*, 2014, **70**, C1437.
36 G. M. Sheldrick, *Acta Crystallogr.*, 2015, **71**, 3–8.
37 G. M. Sheldrick, *Acta Crystallogr.*, 2008, **64**, 112–122.
38 M. C. Burla, R. Caliandro, B. Carrozzini, G. L. Cascarano, C. Giacovazzo, M. Mallamo, A. Mazzone and G. Polidori, *J. Appl. Crystallogr.*, 2014, **48**, 306–309.
39 P. V. D. Sluis and A. L. Spek, *Acta Crystallogr. Sect. A*, 1990, **46**, 194; A. L. Spek, *Acta Crystallogr., Sect. D: Biol. Crystallogr.*, 2009, **65**, 148.
40 C. F. Macrae, P. R. Edgington, P. McCabe, E. Pidcock, G. P. Shields, R. Taylor, M. Towler and J. van de Streek, *J. Appl. Crystallogr.*, 2006, **39**, 453–457.